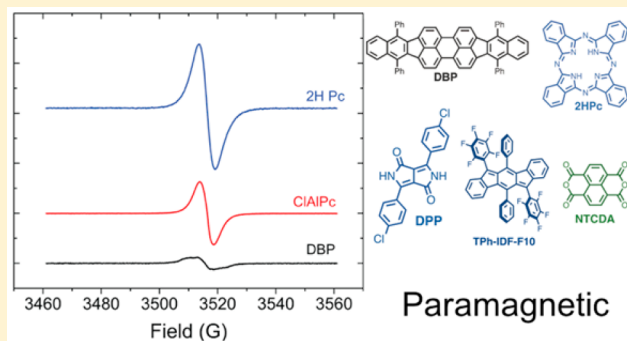# Anomalous Paramagnetism in Closed-Shell Molecular Semiconductors

Gregory P. Eyer,[†] Kevin R. Kittilstved,[‡] and Trisha L. Andrew*,[‡]

[†]University of Wisconsin—Madison, Madison, Wisconsin 53706, United States
[‡]University of Massachusetts—Amherst, Amherst, Massachusetts 01003, United States

S *Supporting Information*

ABSTRACT: Anomalous electron paramagnetic resonance (EPR) signals from formally closed-shell phthalocyanines have been a longstanding mystery. For the past few decades, this illogical observation has remained unexplored because of the belief that it is unique to only the one class of chromophores, namely, phthalocyanines. Here we show that, in fact, a broad structural range of molecular semiconductors, including pentacene, diindenoperylenes, rylene diimides, pyrrolo[c]-pyrroles, and indenofluorenes, show a strong, clear EPR signal (X-band) in the solid state, which is not present in the solution EPR spectra of the same compounds. Further, magnetic susceptibility measurements confirm that these formally closed-shell molecules are paramagnetic (as bulk powders),

even at low temperatures. In some compounds, the intensity of the EPR signal or value of magnetic susceptibility increases after sample purification via physical vapor transport. EPR signal evolution can be directly correlated to the evolution of molecular aggregates. We propose that such anomalous paramagnetism arises from a small concentration of intrinsic radical cations or anions generated through exposure to ambient atmosphere (oxygen, water) and light. The phenomenon described herein notably alters how conjugated molecules/polymers are conceptualized, designed, and processed for nascent magnetoelectronic and magneto-optic applications.

1. INTRODUCTION

Research into molecular organic semiconductors has made great advances toward solving problems in energy and flexible electronics over the past 3 decades.[1,2] In particular, phthalocyanines,[3,4] pentacene,[5] and diindenoperylenes[6,7] are commonplace in a variety of contemporary high-performance, solid-state optoelectronic,[8,9] electronic, and spintronic devices. While these closed-shell molecules are expected to be diamagnetic, selected previous reports describe the mysterious phenomenon of observing an anomalous electron paramagnetic resonance (EPR) signal in—what should be—diamagnetic phthalocyanine samples.[10−14] At the time, these unexpected signals were hypothesized to arise from adsorbed oxygen on crystal faces or at crystal domain boundaries,[10] trapped charges from photodegradation reactions,[11] broken π-bonds,[12] metal impurities,[13] or crystal defect states from thermal treatment.[13,14] However, definitive explanations remained elusive, and further investigations into anomalous paramagnetism in phthalocyanines halted because of the belief that this phenomenon was specific to only one class of material.

In this study, we show that solid-state paramagnetism is, in fact, a common observation across numerous recognizable molecular semiconductors, including pentacene,[5] diindenoperylenes,[6] rylene diimides,[15] indenofluorenes,[16,17] and pyrrolo-[c]pyrroles,[7] which are pervasive photoactive and/or charge-

transporting materials in contemporary organic solar cells, field-effect transistors, and spin valves.[18,19] Because the presence of unpaired electron spin significantly impacts charge carrier lifetime and transport in organic thin films,[20] and because the aforementioned compounds are not expected to demonstrate paramagnetic character, the startling observations reported herein will have broad-ranging implications for designing, handling, and processing organic molecules for nascent spintronic and magneto-optic applications.[21]

2. MATERIALS AND METHODS

The compounds studied were purchased from Sigma-Aldrich (ClAlPc, 85% dye content; 29H, 31H-phthalocyanine, 98% beta; Cl₂SiPc, 85% dye content; NTCDA, 1,4,5,8-napthalenetetracarboxylic dianhydride; pentacene, 99% sublimed; and ZnPc, 97%), Lumtec (DBP, dibenzo-(4,4′,7,7′-tetraphenyl)-diindenoperylene, ~99% sublimed grade; diindenoperylene (DIP), >99% sublimed; PTCBI, 3,4,9,10-perylenetetracarboxylic bisbenzimidazole, >99% sublimed; and SnPc, ~99% sublimed), and TCI (DPP or Pigment Red 254). The indenofluorene compounds (TPh-IDF-F10, TPh-IDF, and
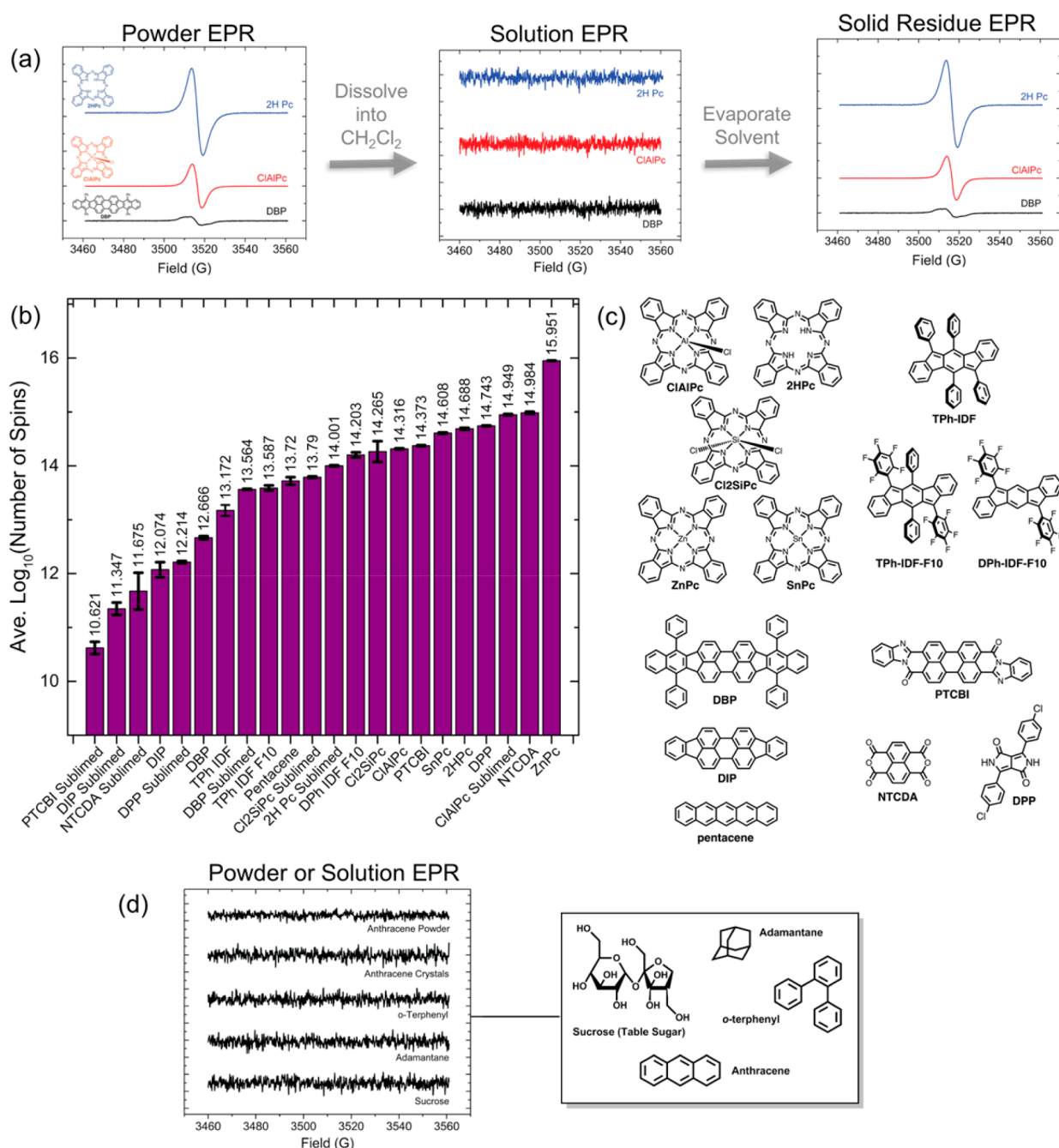
Figure 1. Anomalous paramagnetism in closed-shell organic chromophores. (a) Continuous wave (CW) EPR spectra of selected chromophore powders and dilute solutions of the same chromophores in toluene. An EPR signal is not observed in solutions, which could be due to extreme EPR line width broadening. (b) Spin-counting data for all 14 chromophores (and postsublimation data for eight) plotted as average number of spins on a logarithmic scale with error bars. (c) Chemical structures of the chromophores studied here. (d) Crystalline organic control molecules that do not exhibit an EPR signal in the solid state.

DPh-IDF-F10) were synthesized by a lab member, Dr. Brandon Kobilka, following previously reported procedures[16,17] and purified using flash column chromatography followed by two recrystallizations from ethanol. Teflon-coated spatulas and wax-coated weigh papers were globally used to handle all compounds to prevent introduction of metal contaminants.

Thermal gradient vapor transport (Figure S1 of the Supporting Information) was conducted in a home-built tube furnace with three temperature zones actively heated by high-temperature heating tape wrapped and insulated around the outside tube. The sample (approximately 1 g) was loaded in an interior quartz tube of smaller diameter and placed within the outer, heated tube at the end of the tube opposite the vacuum source and at the same end as the nitrogen inlet. The tube was purged with nitrogen overnight. The following morning, the outer tube was heated under vacuum (using a roughing pump) with a small amount of nitrogen flow to a temperature below decomposition temperature (which was confirmed for each molecule by thermogravimetric analysis) where the sample was placed in zone 1. Because our tube furnace did not have a thermocouple inside to measure temperature in the sublimation zone, temperatures in the table are recorded in °C measured by

an infrared temperature sensor on the outside surface of the heating tape. The conditions for each experiment are listed in Table S1.

After heating, the sublimed sample was isolated between zones 1 and 2, with impurities having been left behind in zone 1 or removed and collected in zone three. All purified samples were analyzed by elemental analysis to confirm their chemical compositions (see Supporting Information). Changes in structure or paramagnetism were not discernible by electron paramagnetic resonance (EPR) or X-ray diffraction due to sublimation with 100% N_2 or 95/5 N_2/H_2 as the flow gas, ruling out potential oxidation reactions during purification.

EPR spectroscopy of solution and powder samples was conducted using a Bruker E500 X-Band (9.8 GHz) Continuous Wave spectrometer equipped with a high-Q cavity at room temperature operated at 0.635 mW microwave energy which corresponds to a signal attenuation of 25 dB. Quartz EPR standard quality tubes with an outer diameter of 4 mm were purchased from Wilmad Lab Glass. A single crystal of 2,2-diphenyl-1-picrylhydrazyl was used as an external field calibration standard. The external field was calibrated before each set of EPR experiments performed on different days. All solution experiments were conducted in degassed solvents (toluene and hexane). All powder experiments were conducted on the neat powder placed inside a glass EPR tube that had been purged with nitrogen and capped. Peak intensities were standardized to the mass of material analyzed. A Bruker Weak Pitch sample was used as an external spin-counting standard (10^{13} spins) to correlate EPR signal intensity to the number of spins present in each powder sample. Spin quantification was performed in triplicate for each sample.

Power saturation experiments were conducted by sweeping across microwave power from 6×10^{-4} mW to 200 mW, acquiring a data point at every whole number microwave attenuation value from 55 to 0 dB. The resulting data was integrated under the EPR absorption curve and the area plotted as peak intensity versus microwave power.

Temperature-dependent magnetic susceptibility values were acquired with a Quantum Design MPMS superconducting quantum interference device (SQUID) susceptometer. Solid samples were weighed and placed inside either Saran Wrap or a gelatin capsule holder before being placed into the magnet bore of the SQUID. Raw data from the magnetometer was processed using the DAVE software program provided by the National Institute of Standards and Technology (NIST).

The DBP radical cation was chemically generated by oxidation of dibenzo-(4,4′,7,7′-tetraphenyl)diindenoperylene (DBP, 54 mg, 0.067 mmol, in 8 mL of dichloromethane) with triethyloxonium hexachloroantimonate[22] (Et_3O^+ $SbCl_6^-$, ~0.015 mg, 3.4×10^{-4} mmol added via a 0.05 mg/mL solution in dichloromethane) in dry, degassed dichloromethane. To this end, a literature prep was adapted to generate just enough radical cation to characterize at a comparative concentration to the powder DBP sample.[22] The solution was sonicated under N_2 for 160 min upon which the solution changed from bright pink to dark purple, and then concentrated via rotary evaporation in the reaction vessel, taking care to avoid exposure to air when possible. The resulting powder was further dried under high vacuum for 10 min, loaded into a quartz EPR tube inside a nitrogen atmosphere glovebox, and analyzed by EPR. For the solution EPR, degassed dichloromethane was added to a small amount of the DBP radical cation powder in a separate quartz tube in the glovebox.

Dynamic light scattering (DLS) experiments were conducted using a Zetasizer Nano with quartz cuvettes with a path length of 5 mm, using a laser wavelength of 632 nm. Standard operating procedures were written for chloroaluminum phthalocyanine aggregates in the 5:1, 5:2, and 5:3 toluene and hexanes solvent systems. All samples and solvents were filtered through 0.4 μm syringe filters prior to data acquisition and great care was taken to prohibit dust from fouling the solutions or cuvettes. Noise filters were applied to selected EPR data from the DLS measurements in Figure 3.

3. RESULTS

We identified anomalous paramagnetic behavior in *powders* of 14 closed-shell molecular organic semiconductors using EPR spectroscopy, including five different phthalocyanines (2HPc, ClAlPc, ZnPc, SnPc, and Cl_2SiPc), two diindenoperylenes (DBP and DIP), three indenofluorenes (TPh-IDF, TPh-IDF-F10, DPh-IDF-F10), pentacene, two rylene diimides (NTCDA and PTCBI), and one pyrrolo[c]pyrrole (DPP). Thoroughly degassed *solutions* of the same compounds showed no observable EPR signal. However, upon concentrating these solutions under an inert atmosphere to remove solvent and retaking an EPR spectrum of the obtained residues, a signal appeared once again. We observed varying average signal intensities between different compounds due to varying concentrations of the hypothesized paramagnetic state. We quantified the relative concentrations of the paramagnetic state in all of these compounds using spin counting with a known standard, and plotted the number of spins on a log scale (Figure 1).

Condensed-phase paramagnetism appeared to be limited to planar organic compounds with extended π-systems. Several other examples of crystalline organic compounds, such as anthracene, adamantane, and sucrose, did not show any solid-state paramagnetism when analyzed by EPR (Figure 1).

The g-values of the observed EPR signals ruled out metal impurities as a potential source of the anomalous signals. The EPR signals also persisted after selected compounds were purified using physical vapor transport (using nitrogen carrier gas, Figure S1). Interestingly, all three n-type (or electron-accepting/-transporting) chromophores studied herein, PTCBI, DPP, and NTCDA, displayed a decrease in the intensity of the observed EPR signal after purification. However, selected p-type (or electron-donating/hole-transporting) chromophores, such as ClAlPc and DBP, displayed an increase in the EPR signal intensity after purification. Replacing inert nitrogen with air in the sample tube did not appreciably affect EPR signal intensity (Figure S2 and Table S2), meaning that any oxidation resulting from air exposure was already at a steady state or did not occur at all.

The magnetic susceptibilities of selected, closed-shell compounds were measured using a superconducting quantum interference device (SQUID) magnetometer. Figure 2 shows the calculated χT versus T curves for six samples obtained after applying a systematic diamagnetic correction to account for the sample holder. Consistent with the anomalous EPR signals described above, all investigated samples displayed well-behaved paramagnetic characteristics, even at low temperatures, despite being closed-shell. The magnetic susceptibility of an admixture of the stable organic radical TEMPO (spin = 1/2) and ClAlPc was also measured as a reference. TEMPO is known to demonstrate paramagnetic behavior above 4 K;[23] the curve shown in Figure 2 is consistent with this behavior. The
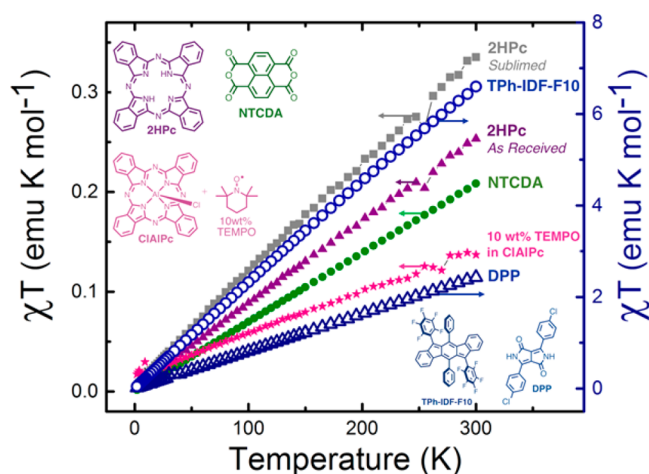
Figure 2. Magnetic susceptibility measurements of selected closed-shell chromophores. For clarity, the χT values for DPP and TPh-IDF-F10 are plotted on a separate (right) axis.

Figure 3. Aggregation-dependent evolution of paramagnetic EPR signal for ClAlPc. (a) Observing increasing ClAlPc aggregate size in various solvent/nonsolvent mixtures via dynamic light scattering measurements. (b) Correlated EPR spectra in various solvent/nonsolvent mixtures.

phthalocyanine 2HPc retained its paramagnetism after purification, supporting the conclusion that the observed magnetic behavior is not caused by extrinsic impurities. Notably, NTCDA and the indenofluorene compound TPh-IDF-F10 displayed high χT values.

Since unexpected paramagnetism seemed to be an exclusively condensed-phase phenomenon, we sought to observe, to the best of our ability, the evolution of the magnetic signal with controlled molecular aggregation (Figure 3). We started with a dilute solution of ClAlPc in toluene, in which ClAlPc is partially soluble, and added discrete amounts of hexanes, in which ClAlPc is insoluble, to cause precipitation of nanoscale aggregates. EPR spectra were measured for each discrete solvent mixture (Figure 3) and dynamic light scattering (DLS) experiments were concomitantly performed to confirm the formation of scattering aggregates. Our experiments clearly revealed that a discernible EPR signal is observable only upon aggregation of ClAlPc molecules.

The strengths of the observed paramagnetic signals for ClAlPc and DBP were also quantified (using spin counting) before and after sample purification by thermal gradient vapor transport (simply called "sublimation" henceforth).[24−30] EPR signal intensity increased after purification for both samples. Powder samples of ClAlPc displayed a 4.9× increase in integrated signal intensity after sublimation and powder samples of DBP displayed a 7.9× increase in integrated signal intensity after sublimation (see Figure 1b). In contrast, all the three *n*-type molecules studied herein displayed decreases in EPR signal intensity upon sublimation. Carbon-centered anions are comparatively less stable than carbon-centered cations, and therefore, any radical anions present in PTCBI, NTCDA, and DPP would be easier to remove upon thermal treatment under an inert atmosphere compared to any radical cations present in pentacene, DBP, or a phthalocyanine. Further, thermal annealing and purification via physical vapor transport are known to increase the size of tightly packed crystalline aggregates in PTCBI, NTCDA, and DPP,[15,31] which should lead to reduced penetration of oxygen/water into the samples and, therefore, suppress creation of charged radical species.

We also compared the observed EPR signal arising from sublimed closed-shell DBP powders to that of its chemically generated[22] radical cation (Figure 4, Figure S3). The powder
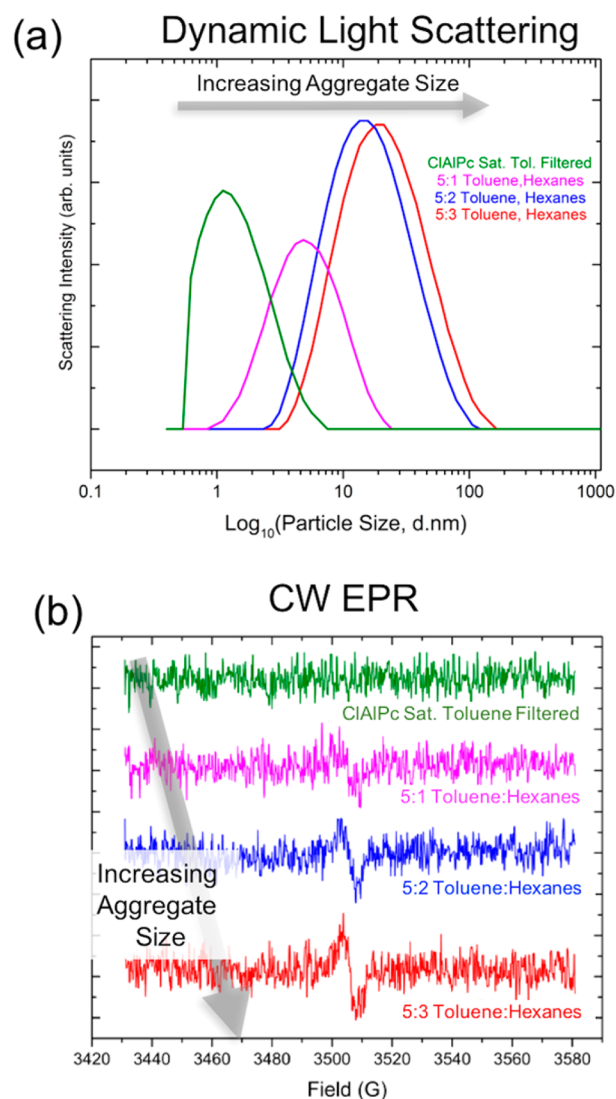
EPR spectrum of DBP was much broader than that of its chemically generated radical cation. The g-values of the DBP signal and the radical cation signal were also distinct (Figure S4). In solution, the radical cation displayed a persistent, sharp EPR signal but no signal was observed for DBP solutions. Upon partial reduction of the DBP radical cation powder with hydrazine vapor, a mixed EPR signal was observed, which could be decomposed to the broad signal arising from neutral DBP and the sharp peak of its radical cation.

Variable temperature CW EPR experiments were also conducted on powders of DBP and its radical cation (Figure S5). The integrated peak area for both samples increased with lowered temperatures. This notable change in peak integration with decreasing temperature further confirms that the observed paramagnetism in DBP is an intrinsic characteristic and does not arise from external impurities.[32]

Microwave power saturation studies at 100 K (Figure S6) revealed that the DBP signal saturated more quickly than its radical cation. This indicates that the source of paramagnetism
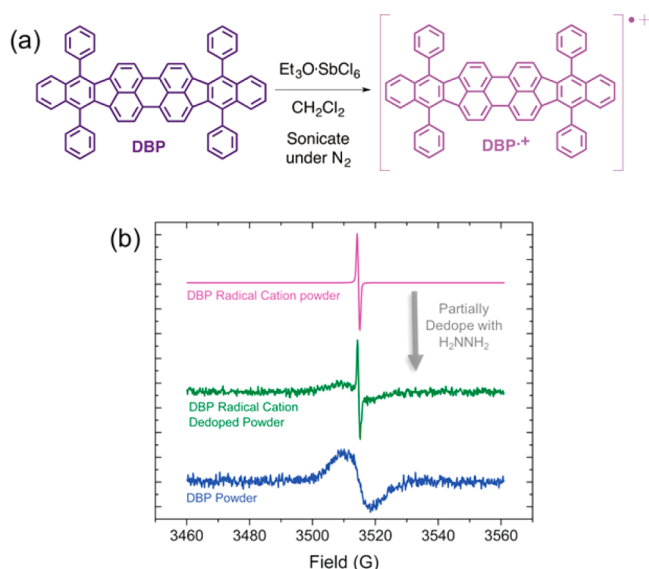
Figure 4. Generation (a) and dedoping (compensation) of the chemical generated DBP radical cation sample. We see in the powder EPR spectra (b) that the sharp signal from the chemically generated radical cation is distinct from the intrinsic paramagnetic state in the DBP powder.

in DBP cannot relax as quickly as the unpaired spin in the chemically generated DBP radical cation.

4. DISCUSSION

We posit that the anomalous condensed-phase paramagnetic states in the 14 closed-shell chromophores studies herein arise from a small (subppm) concentration of intrinsic radical cations or anions generated through exposure to ambient atmosphere (oxygen, water) and light, which can delocalize throughout the molecules' extended π-systems. On the basis of the well-known chemical and redox behavior of the 14 compounds studied herein, it is likely that the phthalocyanines, diindenoperylenes, and pentacene are photo-oxidized (due to their comparatively high-lying HOMOs), whereas the rylene diimides and pyrrolo-[c]pyrrole are photoreduced (due to their comparatively low-lying LUMOs). While we took great care to eliminate or minimize exposure of the samples to oxygen/water and room light, we cannot plausibly deny that a small amount of photo-oxidation or photoreduction occurred during handling. In small enough concentrations, the charged radicals could be outside the detection range of our EPR spectrometer for solution samples, or result in a very broad signal that is not easily visualized by X-Band (9.8 GHz) EPR. Because redox reactions from crystal surfaces occur faster than isolated molecules in solution (due to a higher density of states in the condensed phase),[32] it is also possible that the posited charged radicals are formed only in the solid state. These proposed explanations are consistent with the aggregation study presented in Figure 3, where low concentrations of charged radical species could simply not be formed and/or detected until aggregates evolve. The hypothesis of a dilute radical cation is also in agreement with the experiment where purging the EPR tube with air or oxygen did not affect the magnitude of the EPR signal: if the solid-state redox reactions had already progressed as far as they were able, or to an equilibrium state, then further increases in EPR signal intensity should not occur.

The differences in total spin concentration in ClAlPc and DBP before and after sublimation can also be explained by the evolution of charged radical species from exposure to ambient atmosphere and light during the sublimation process. All the three n-type molecules studied herein displayed decreases in EPR signal intensity upon sublimation. Thermal annealing and purification via physical vapor transport are known to increase the size of tightly packed crystalline aggregates in PTCBI, NTCDA, and DPP,[15,31] which should lead to reduced penetration of oxygen/water into the samples and, therefore, suppress creation of charged radical species.

Powders of the chemically generated DBP radical cations contain a high density of unpaired spins, much higher than we posit is created upon simple ambient photo-oxidation of DBP. This discrepancy explains the significant difference in EPR signal line widths between powders of neutral DBP and its chemically generated radical cation. The smaller EPR line width of radical cation powders is caused by spatial localization of each radical due to Coulombic repulsion between adjacent charged radicals at high volumetric spin densities. In contrast, due to a lower concentration of unpaired spins in the neutral DBP sample, we believe that the ambient-generated radical cation is less spatially constrained and able to delocalize over a larger number of molecules, thus interacting with a larger number of hydrogen hyperfine fields that broaden the EPR signal. Consistent with this explanation, the EPR signal of the chemically generated radical cation broadens upon partial dedoping with hydrazine vapor—when the volumetric spin density decreases upon dedoping, individual radical cations can delocalize over longer distances.

A low concentration of unpaired spins also explains why the samples retain paramagnetic character at low temperatures (Figure 2). High concentrations of localized spins should lead to spin pairing and diamagnetic behavior at reduced temperatures. At low concentrations, however, spin pairing is unlikely and delocalized radical cations should effectively behave as noninteracting paramagnets, similar to the case of a discrete organic radical, TEMPO, mixed into ClAlPc powders.

The observed paramagnetism of the indenofluorene TPh-IDF-F10 is particularly interesting. Wu and co-workers reported the synthesis and characterization of structurally similar compounds, whose unique magnetic properties arise due to the significant presence of an open-shell diradical resonance structure.[33] Wu's molecules consistently display diamagnetic behavior at low temperatures due to intramolecular spin pairing, which transitions to paramagnetic behavior past ca. 200 K. In sharp contrast, the IDFs studies herein do not display any diamagnetic behavior, suggesting that different electron-spin interactions are at play.

5. CONCLUSIONS

In this report, we discuss our startling observation that many recognizable molecular organic semiconductors display paramagnetic behavior despite being closed-shell systems. Both EPR spectroscopy and SQUID magnetometry reveal that phthalocyanines, pentacene, rylene diimides, indenofluorenes, and a pyrrolo[c]pyrrole display clear paramagnetic characteristics in the solid state, which disappears in dilute solutions of the same compounds. We posit that paramagnetism in these compounds arises due to the presence of a small concentration of charged radical species (radical cations or anions) generated upon exposure to ambient atmosphere (oxygen, water) and light. High volumetric densities of charged radical species in a

solid sample (created via chemical oxidation) lead to significant localization of unpaired spin, with immediate spin delocalization observed upon partial destruction (by dedoping) of the charged radical species.

Our work provides crucial insights into future best practices for fabricating spintronic and magneto-optic devices. The presence of a persistent charged radical species in thin films of molecular semiconductors must be addressed while explaining magnetoresistive effects in solid-state spin valves. The presence of charged radical species could alter the desired or predicted electronic and magnetic behavior of a particular molecule and contaminate device characteristics.

The total unpaired spin concentration in thin films of molecular semiconductors must be kept low to suppress spin–spin scattering and increase the average coherence length of unpaired spins in the sample. Furthermore, we suggest that high concentrations of charged radical species, such as polarons, which are pervasive in solid-state organic electronic devices, will also lead to localization of discrete unpaired spins and therefore suppression of any magnetic properties that may otherwise be displayed by thin films of molecular semiconductors. Therefore, care must be taken while analyzing electrical characterization data from spintronic devices, such as spin valves, to account for spin–polaron interactions.

■ ASSOCIATED CONTENT

Ⓢ Supporting Information

The Supporting Information is available free of charge on the ACS Publications website at DOI: 10.1021/acs.jpcc.7b07270.

General methods, further discussion, and control experiment data (PDF)

■ AUTHOR INFORMATION

Corresponding Author
*E-mail: tandrew@umass.edu.

ORCID Ⓘ
Kevin R. Kittilstved: 0000-0002-9852-7454
Trisha L. Andrew: 0000-0002-8193-2912

Author Contributions
G.P.E. executed all experiments, except SQUID magnetometry, which was carried out by K.R.K. G.P.E. and T.L.A. analyzed the data and wrote the manuscript.

Notes
The authors declare no competing financial interest.

■ ACKNOWLEDGMENTS

■ REFERENCES

(1) Tang, C. W. Two-Layer Organic Photovoltaic Cell. *Appl. Phys. Lett.* **1986**, *48*, 183–185.

(2) Service, R. F. Outlook Brightens for Plastic Solar Cells. *Science* **2011**, *332*, 293.

(3) Melville, O. A.; Lessard, B. H.; Bender, T. P. Phthalocyanine-Based Organic Thin-Film Transistors: A Review of Recent Advances. *ACS Appl. Mater. Interfaces* **2015**, *7*, 13105–13118.

(4) Barraud, C.; Bouzehouane, K.; Deranlot, C.; Kim, D. J.; Rakshit, R.; Shi, S.; Arabski, J.; Bowen, M.; Beaurepaire, E.; Boukari, S.; et al. Phthalocyanine Based Molecular Spintronic Devices. *Dalton Trans.* **2016**, *45*, 16694–16699.

(5) Kitamura, M.; Arakawa, Y. Pentacene-Based Organic Field-Effect Transistors. *J. Phys.: Condens. Matter* **2008**, *20*, 184011.

(6) Wagner, J.; Gruber, M.; Hinderhofer, A.; Wilke, A.; Bröker, B.; Frisch, J.; Amsalem, P.; Vollmer, A.; Opitz, A.; Koch, N.; et al. High Fill Factor and Open Circuit Voltage in Organic Photovoltaic Cells with Diindenoperylene as Donor Material. *Adv. Funct. Mater.* **2010**, *20*, 4295–4303.

(7) Peng, Y.; Zhang, L.; Andrew, T. L. High Open-Circuit Voltage, High Fill Factor Single-Junction Organic Solar Cells. *Appl. Phys. Lett.* **2014**, *105*, 083304.

(8) Verreet, B.; Müller, R.; Rand, B. P.; Vasseur, K.; Heremans, P. Structural Templating of Chloro-Aluminum Phthalocyanine Layers for Planar and Bulk Heterojunction Organic Solar Cells. *Org. Electron.* **2011**, *12*, 2131–2139.

(9) Chauhan, K. V.; Sullivan, P.; Yang, J. L.; Jones, T. S. Efficient Organic Photovoltaic Cells Through Structural Modification of Chloroaluminum Phthalocyanine/Fullerene Heterojunctions. *J. Phys. Chem. C* **2010**, *114*, 3304–3308.

(10) Raynor, J. B.; Robson, M.; Torrens-Burton, A. S. M. Origin of the Electron Spin Resonance Signal in Diamagnetic Phthalocyanins. *J. Chem. Soc., Dalton Trans.* **1977**, *23*, 2360–2364.

(11) Harbour, J. R.; Loutfy, R. O. An Electron Spin Resonance Investigation into Dark and Light-Induced Paramagnetism in Metal-Free Phthalocyanines. *J. Phys. Chem. Solids* **1982**, *43*, 513–520.

(12) Winslow, F. H.; Baker, W. O.; Yager, W. A. *J. Am. Chem. Soc.* **1955**, *77*, 4751–4756.

(13) Assour, J. M.; Harrison, S. E. On the Origin of Unpaired Electrons in Metal-Free Phthalocyanines. *J. Phys. Chem.* **1964**, *68*, 872–876.

(14) Wagner, H. J.; Loutfy, R. O.; Hsiao, C.-K. Purification and Characterization of Phthalocyanines. *J. Mater. Sci.* **1982**, *17*, 2781–2791.

(15) Zhan, X.; Facchetti, A.; Barlow, S.; Marks, T. J.; Ratner, M. A.; Wasielewski, M. R.; Marder, S. R. Rylene and Related Diimides for Organic Electronics. *Adv. Mater.* **2011**, *23*, 268–284.

(16) Chase, D. T.; Rose, B. D.; McClintock, S. P.; Zakharov, L. N.; Haley, M. M. Indeno[1,2-b]fluorenes: Fully Conjugated Antiaromatic Analogues of Acenes. *Angew. Chem., Int. Ed.* **2011**, *50*, 1127–1130.

(17) Nishida, J.; Tsukaguchi, S.; Yamashita, Y. Synthesis, Crystal Structures and Properties of 6,12-Diaryl-Substituted Indeno[1,2-b]fluorenes. *Chem. - Eur. J.* **2012**, *18*, 8964–8970.

(18) Zhang, X.; Ma, Q.; Suzuki, K.; Sugihara, A.; Qin, G.; Miyazaki, T.; Mizukami, S. Magnetoresistance Effect in Rubrene-Based Spin Valves at Room Temperature. *ACS Appl. Mater. Interfaces* **2015**, *7*, 4685–4692.

(19) Dediu, A. A.; Hueso, L. E.; Bergenti, I.; Taliani, C. Spin Routes in Organic Semiconductors. *Nat. Mater.* **2009**, *8*, 707–716.

(20) Rao, A.; Chow, P. C. Y.; Gélinas, S.; Schlenker, C. W.; Li, C.-Z.; Yip, H.- L.; Jen, A. K. Y.; Ginger, D. S.; Friend, R. H. The Role of Spin in the Kinetic Control of Recombination in Organic Photovoltaics. *Nature* **2013**, *500*, 435–439.

(21) Swager, T. M. 50th Anniversary Perspective: Conducting/Semiconducting Conjugated Polymers. A Personal Perspective on the Past and the Future. *Macromolecules* **2017**, *50*, 4867–4886.

(22) Rathore, R.; Kumar, A. S.; Lindeman, S. V.; Kochi, J. K. Preparation and Structures of Crystalline Aromatic Cation-Radical Salts. Triethyloxonium Hexachloroantimonate as a Novel (One-Electron) Oxidant. *J. Org. Chem.* **1998**, *63*, 5847–5856.

(23) Kavala, M.; Boča, R.; Dlháň, L.; Brezová, V.; Breza, M.; Kozisek, J.; Fronc, M.; Herich, P.; Svorc, L.; Szolcsanyi, P. Preparation and Spectroscopic, Magnetic, and Electrochemical Studies of Mono-/Biradical TEMPO Derivatives. *J. Org. Chem.* **2013**, *78*, 6558–6569.

(24) Mao, H. Y.; Wang, R.; Wang, Y.; Niu, T. C.; Zhong, J. Q.; Huang, M. Y.; Qi, D. C.; Loh, K. P.; Wee, A. T. S.; Chen, W. Chemical Vapor Deposition Graphene as Structural Template to Control Interfacial Molecular Orientation of Chloroaluminum Phthalocyanine. *Appl. Phys. Lett.* **2011**, *99*, 093301.

(25) Basova, T. V.; Kiselev, V. G.; Dubkov, I. S.; Latteyer, F.; Gromilov, S. A.; Peisert, K.; Chassè, T. Optical Spectroscopy and XRD Study of Molecular Orientation, Polymorphism, and Phase Transitions Fluorinated Vanadyl Phthalocyanine Thin Films. *J. Phys. Chem. C* **2013**, *117*, 7097−7106.

(26) Vasseur, K.; Rand, B. P.; Cheyns, D.; Temst, K.; Froyen, L.; Heremans, P. Correlating the Polymorphism of Titanyl Phthalocyanine Thin Films with Solar Cell Performance. *J. Phys. Chem. Lett.* **2012**, *3*, 2395−2400.

(27) Li, L.; Tang, Q.; Li, H.; Yang, X.; Hu, W.; Song, W.; Shuai, Z.; Xu, W.; Liu, Y.; Zhu, D. An Ultra Closely π-Stacked Organic Semiconductor for High Performance Field-Effect Transistors. *Adv. Mater.* **2007**, *19*, 2613−2617.

(28) Bayliss, S. M.; Heutz, S.; Rumbles, G.; Jones, T. S. Thin Film Properties and Surface Morphology of Metal Free Phthalocyanine Films Grown by Organic Molecular Beam Deposition. *Phys. Chem. Chem. Phys.* **1999**, *1*, 3673−3676.

(29) Heutz, S.; Bayliss, S. M.; Middleton, R. L.; Rumbles, G.; Jones, T. S. Polymorphism in Phthalocyanine Thin Films: Mechanism of the α -> β Transition. *J. Phys. Chem. B* **2000**, *104*, 7124−7129.

(30) Debad, J. D.; Morris, J. C.; Lynch, V.; Magnus, P.; Bard, A. J. Dibenzotetraphenylperiflanthene: Synthesis, Photophysical Properties, and Electrogenerated Chemiluminescence. *J. Am. Chem. Soc.* **1996**, *118*, 2374−2379.

(31) Lunt, R. R.; Benziger, J. B.; Forrest, S. R. Growth of an Ordered Organic Heterojunction. *Adv. Mater.* **2007**, *19*, 4229−4233.

(32) Rathore, R.; Abdelwahed, S. H.; Kiesewetter, M. K.; Reiter, R. C.; Stevenson, C. D. Intramolecular Electron Transfer in Cofacially π-Stacked Fluorenes: Evidence of Tunneling. *J. Phys. Chem. B* **2006**, *110*, 1536−1540.

(33) Sun, Z.; Zeng, Z.; Wu, J. Zethrenes, Extended p-Quinodimethanes, and Periacenes with a Singlet Biradical Ground State. *Acc. Chem. Res.* **2014**, *47*, 2582−2591.